Quaternary Research 79 (2013) 228–241

Contents lists available at SciVerse ScienceDirect

Quaternary Research

journal homepage: www.elsevier.com/locate/yqres

Depositional processes of reworked tephra from the Late Pleistocene Youngest Toba Tuff deposits in the Lenggong Valley, Malaysia

Emma Gatti [a,*], Mokhtar Saidin [b], Khairunnisa Talib [b], NurAsikin Rashidi [b], Philip Gibbard [a], Clive Oppenheimer [a]

[a] Department of Geography, Downing Place, CB2 3EN, University of Cambridge, Cambridge, UK
[b] Centre for Global Archaeological Research, Universiti Sains Malaysia, Penang 11800, Malaysia

ARTICLE INFO

Article history:
Received 6 April 2012
Available online 23 December 2012

Keywords:
Youngest Toba Tuff
Primary tephra
Reworked tephra
Fluvial stratigraphy
Particle size
Mineralogy
Paleoenvironmental reconstructions
Lenggong valley
Malaysia

ABSTRACT

Two fundamental issues for tephrostratigraphic work are the differentiation of primary from reworked tephra and the characterization of reworking mechanisms. We study the depositional processes of four deposits of Youngest Toba Tuff in the Lenggong valley, Malaysia. We focus on site stratigraphy, particle-size distributions, magnetic susceptibility and mineralogical associations. Reworked tephra display variable sedimentological characteristics including polymodal and unimodal, very fine to coarse-grained distributions, and variable concentrations of ash. Particle-size distributions from this study are similar to published analyses for primary deposits, demonstrating that particle size alone cannot distinguish primary from secondary tephra. The tephra sequences are associated with fluvial and colluvial deposition. Three facies are identified: flood flow, mudflow and slumping. The ash accumulated rapidly, over a period of a few days to months. In this valley the ideal site for paleoenvironmental reconstructions is Kampung Luat 3, where ash accumulated at least in two distinct phases. Despite the rapid accumulation, the Lenggong sites are not well-suited for paleoenvironmental studies of the YTT impact. The time lag between the primary deposition and the floods is unknown and the records could have been modified by site-specific characteristics. Such variables should be considered when proposing paleo-environmental reconstructions based on reworked tephra.

Introduction

Distal tephra deposits can be used to correlate a wide variety of palaeo-records over ranges of up to thousands of kilometers (Sarna-Wojcicki et al., 1985). Tephrostratigraphy and tephrochronology, including the study of microtephra, therefore represent an important complement to paleoenvironmental and archaeological reconstructions (Sarna-Wojcicki and Davis, 1991; Alloway et al., 2007; Lowe, 2011; Davies et al., 2012) because they potentially provide easily-identified, isochronous markers. However, before being used in this way, their integrity should be carefully assessed. Only primary deposits (i.e., in situ ashfall deposits) should be used for high-resolution chronological reconstructions, since only ash immediately deposited after the eruption can guarantee temporal continuity between the pre- and post-eruption facies. Distinguishing primary from secondary deposits (i.e., those arising from reworking of primary ash materials) is therefore a fundamental step before assuming that encasing sediments represent pre- and post-eruptive periods (Schneider et al., 2001). To this end, several solutions have been proposed. From assessments of the percentage of ash grains and the presence or absence of micro-scale structures indicating fluid reworking, Morley and Woodward (2011) inferred primary versus secondary deposits. Jones (2010) studied the particle-size distributions of primary and reworked ash units at Jwalapuram in India. She noticed that the lowermost primary ash was finer grained than all other ash samples, and suggested that such a particularly fine-grained composition resulted from sorting of the ash fallout during gentle redeposition into an aquatic environment. Overall, in the majority of studies the differences between primary and secondary ash are assessed through a combination of micro-scale and macro-scale semi-quantitative observations, adapted to each case.

While reworked deposits may not provide reliable temporal markers, they can still be valuable in paleoenvironmental studies, such as in the investigation of the environmental impact of ash fallout on the receiving environment. Proxies, including pollen, phytoliths, benthic organisms and geochemical traces from sediments, have been used previously for assessing post-eruptive environmental changes (Schulz et al., 2002; Margari et al., 2007; Williams et al., 2009; Haslam et al., 2010). However, before reworked tephra deposits can be used in paleoenvironmental studies, it is critical to understand and reconstruct their depositional history and transport pathways.

Traditional environmental records provided by geochemical and paleontological proxies are usually extracted from high-resolution sedimentary sequences which have established temporal records, such as lake beds, varve and loess (Lowe and Walker, 1984). In the

* Corresponding author.
E-mail address: eg322@cam.ac.uk (E. Gatti).

0033-5894/$ – see front matter
http://dx.doi.org/10.1016/j.yqres.2012.11.006

case of tephrostratigraphical sections, the resolution of the sediments deposited is too low to be distinguished temporally (Williams, 2012a). The question is, therefore: can environmental proxies reliably record the environmental changes that occurred during and after the ashfall event? The first step in addressing this question is to understand the depositional pathway that resulted in the formation of the tephra unit, in order to select the best site for paleoenvironmental reconstruction. Errors can arise where gaps occur in the episodes of accumulation as a consequence of non-deposition, local erosion and/or low sediment yields. The high variability of the sedimentological characteristics of the reworked tephra—even when the ash is deposited in the same environment—can potentially complicate further the reconstruction of the reworking processes (Davies et al., 2007; Pyne-O'Donnell, 2011; Davies et al., 2012).

This article focuses on these two issues, an attempt to distinguish between primary and secondary ash and an assessment of the mechanisms of tephra reworking. For this purpose, the research analyses four newly discovered Youngest Toba Tuff (YTT) tephra exposures at Lenggong, in Malaysia (Fig. 1), in addition to presenting new geochemical data on the glass shards that confirm that the tephra corresponds to the YTT. The aims are: a) to determine whether it is possible, using the methods presented (see below), to distinguish between primary and secondary ash; and b) to determine the most suitable site in the Lenggong valley for future paleoenvironmental reconstruction. The YTT horizons provide an ideal case for the study of secondary ash deposits because of their thickness and spatial distribution. Moreover, the impact of the YTT ashfall on global climate, environment and human population is still widely debated.

The YTT eruption and its potential environmental and human impact

The ~73 ka super-eruption of Toba, a 'supervolcano' in northern Sumatra, is the largest known eruption of the Quaternary (Chesner and Rose, 1991; Oppenheimer, 2002). Its crudely estimated magnitude is 8.8 (Mason et al., 2004), equivalent to 7×10^{15} kg (or 2800 km^3 dense rock equivalent, DRE) of rhyolitic magma (Rose and Chesner, 1990; Chesner and Rose, 1991; Chesner et al., 1991). The volume of co-ignimbrite ash fallout has been estimated as 800–1500 km^3 DRE (Rose and Chesner, 1987, 1990; Matthews et al., 2012; Gatti and Oppenheimer, 2012). The eruption is dated using $^{40}Ar/^{39}Ar$ to 73 ± 4 ka (Chesner et al., 1991), and it is considered the youngest of three major Quaternary eruptive events that produced characteristic rhyolitic tuffs associated with the Toba caldera (Chesner et al., 1991). Terrestrial YTT tephra have been identified from several sites in India and offshore in the Bay of Bengal (Korisettar et al., 1988; Acharyya and Basu, 1993; Kale et al., 1993; Shane et al., 1995; Westgate et al., 1998), Malaysia (Ninkovich, 1979; Rose and Chesner, 1990; Shane et al., 1995) and possibly Bangladesh (Acharyya and Basu, 1993).

The extraordinary extent of the ashfall has provoked many hypotheses regarding the potential climatic, environmental and paleoanthropological impacts of the eruption (Rampino and Self, 1992, 1993; Zielinski et al., 1996; Ambrose, 1998; Schulz et al., 2002; Gathorne-Hardy and Harcourt-Smith, 2003; Williams et al., 2009; Haslam and Petraglia, 2010; Williams et al., 2010; Jones, 2012; Oppenheimer, 2012; Petraglia et al., 2012; Williams, 2012a,b).

The questions and hypotheses regarding the environmental impact of the YTT are still debated, and the principal importance of the distal tephra deposits lies in their application in establishing the impact of the ashfall on local environments (Petraglia et al., 2007; Jones and Pal, 2009; Williams et al., 2009; Haslam et al., 2010; Jones, 2010; Gatti et al., 2011; Blinkhorn et al., 2012). For example, Ambrose (2003) and Williams et al. (2009) have used the distal YTT deposits in the Son Valley, India, to extract stable carbon isotopes from carbonate nodules found both above and beneath the ash. They interpreted their results as revealing a decrease in C_4 and increase in C_3 plants, immediately following the YTT, substantiating the conclusion that the ashfall caused a local vegetational change from trees to open grassland. Likewise, Haslam et al. (2010) used a similar procedure on a YTT deposit from south central India and found the same dramatic climatic shift towards drier/cooler conditions immediately following the eruption. These authors further suggested that such an environmental shift persisted for at least several centuries (Haslam et al., 2010).

Nevertheless, there is no general consensus around the environmental impact of the YTT ashfall. The initial hypotheses are strongly challenged by the lack of clear evidence of long-term global environmental shock (cf. van der Kaars et al., 2012). Recent studies have questioned several procedural issues in the methods used to reach these conclusions. For example, recent work of Blinkhorn et al. (2012) re-assessed the results in Haslam et al. (2010) and suggested that the isotope variations recorded in the vertical columns were related to the local morphology of each site, rather than the volcanic impact of the ashfall on the environment. Therefore, a study focused on the significance of the tephra sequences and the implications of their taphonomic characteristics seems timely.

The Lenggong valley (Fig. 1) is well known as a locality where YTT tephra deposits can be found (Scrivenor, 1930; Ninkovich et al., 1978; Ninkovich, 1979; Chesner et al., 1991). The most studied YTT site in the valley is Kota Tampan, a locality where the ash has been used as an isochronous marker for assessing the age of the sediments and their associated stone tools. Here a ^{14}C date of ~35 ^{14}C ka BP was obtained for the sediments immediately underlying the ash, the latter including the Tampan Palaeolithic tools (Stauffer, 1973). Later, Ninkovich et al. (1978) characterized the ash by geochemical fingerprinting, confirming it to be the YTT, and thus reinterpreted the age of the Tampanian tools to ~75 ka. Although the Lenggong valley tephra have been geochemically characterized and identified as YTT (e.g., Mokhtar, 2009; Smith et al., 2011; Matthews et al., 2012), to the authors' knowledge, no accurate stratigraphic studies exist concerning the nature and geological significance of the Lenggong tephra. Furthermore, it is unknown whether the YTT ash at Kota Tampan is a primary or reworked deposit.

Study area

The Lenggong valley (Fig. 1) is located in the Perak district of north Peninsular Malaysia, 350 km from the Toba caldera. The Perak River is ~400 km long and is associated with a gently northeast to southwest-sloping terrain (Morgan, 1973). Beyond the artificial lake of Kampong Kuala Benderok and the Temenggor dam, the Perak River has a relatively constant gradient of ~0.8 m/km. The Lenggong valley is ~40 km long and ~2–4 km wide, constrained between the deeply dissected slopes in the Main Range Granite, a post-Triassic acid pluton (Stauffer, 1972), through which the river has incised. The overlying Quaternary sequences of south Perak comprise four alluvial deposits that characterize the inland valley fill (Walker, 1956; Stauffer, 1972): in ascending chronological order they are the *Boulder beds*, the *Old Alluvium* (Middle Pleistocene), the *Young Alluvium* (from the last interglacial to present) and *Organic mud and peat* (Holocene).

Geomorphological setting of the sites investigated

Four sites were investigated in 2010 (Fig. 2), located near Lenggong village (5° 7′ 42.52″ N, 100° 59′ 34.35″ E), 60 km north from the capital of Perak Ipoh. The terrain is mostly covered by rainforest. The Kampung Luat sites (Figs. 2a and b) occur near the main channel of the Perak River. Sites Kampung Luat 1 and Kampung Luat 2 (KgL1 and KgL2) occur, respectively, on the eastern bank of the river, 289 m and 212 m from the main channel. They are located at 69 and 68 m asl, or 4 and 3 m above the main channel. They are currently sited at the margins of an artificial lake. The base of the ash was obscured, and the top was truncated by the modern soil.

https://doi.org/10.1016/j.yqres.2012.11.006 Published online by Cambridge University Press

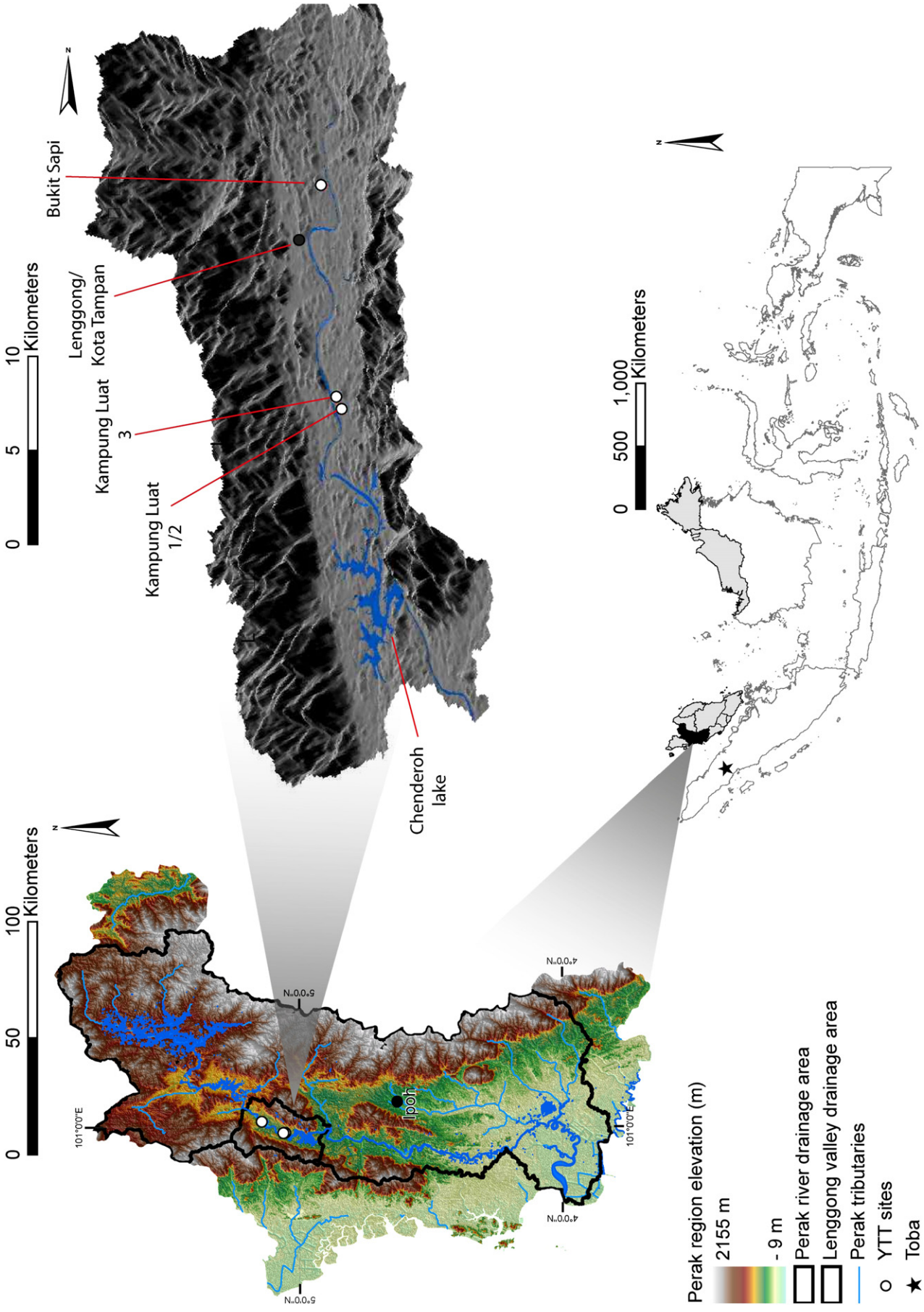

Figure 1. Map of the Perak River region, northwest Peninsular Malaysia. The Perak region is bounded to the north by the Thailand border and Kedah County, east by the Malaysian counties of Kelantan and Pahang, west by the Malaccan Strait, and south by the Selangor region. The Lenggong valley is geomorphologically composed of the dissected hill slopes of the Main Range Granite (Stauffer, 1972) and the alluvial Quaternary sediments of the Perak floodplain. Toba is ~350 km from the Lenggong valley. ASTER DEM of the region obtained from GDEM (ASTER GDEM is a product of METI and NASA).

https://doi.org/10.1016/j.yqres.2012.11.006 Published online by Cambridge University Press

Figure 2. YTT sites in the Lenggong valley. a) Kampung Luat 1 (KgL1); b) Kampung Luat 2 (KgL2); c) Kampung Luat 3 (KgL3); d) Bukit Sapi.

Kampung Luat 3 (KgL3, Fig. 2c) is located on a well-preserved fluvial terrace on the right-hand side of the main channel. The ash is preserved at an altitude of 71 m asl, 115 m from the main channel and at 11 m above the Perak River bed. The ash units lie at the top of the fluvial terrace deposits, exposed during a quarry excavation. No deposits overlie the tephra at this locality, the surface of the ash being colonised by dense rainforest vegetation.

The unit exposed at Bukit Sapi (BTS, Fig. 2d) occurs at an altitude of 79 m asl. The site is 470 m distant from the main channel and 14 m above the river bed. It is part of a small tributary stream valley incised into the northwestern side of the Perak River valley. Neither the bottom nor the top of the sequence could be seen because of the vegetation cover.

Methodology

Ash samples were collected at different intervals, depending on the structures and type of sediments occurring within the sequences. Facies interpretations are based on the depositional models of Nakayama and Yoshikawa (1997) and Kataoka (2005).

Geochemistry

The samples were cleaned in deionised water and left in a warm ultrasonic bath for 10 min. Then, 20–30 grains in the fraction 63–125 μm were mounted, impregnated, polished and gold-coated for electron probe analyses.

An electron probe (EPMA) Cameca SX-100 was used to obtain the major element geochemical fingerprints for the ash units. A beam current at 15 keV 2 nA was applied to measure the Na, Si, K, Ca, Ti, Fe, Al and Mg content. Na was counted early to minimise loss of this element. The analyses were normalised excluding water. International standard silica glass (O = 48.1 wt%, Si = 34.9 wt%) was used as a reference.

Trace element compositions of individual glass shards were measured using a New Wave UP213 Nd:YAG laser ablation system interfaced to

https://doi.org/10.1016/j.yqres.2012.11.006 Published online by Cambridge University Press

a Perkin-Elmer Elan DRC II ICP-MS (Westgate et al., 1994). The laser beam had a 60-μm diameter, a repetition rate of 10 Hz and power of ~0.2 mJ. NIST 610 (National Institute of Standards and Technology, Gaithersburg, Maryland, USA) was applied for calibration of element sensitivity. CaO was used for internal standard normalisation.

Sedimentology

Samples were cleaned to remove secondary carbonates using 5% HCl and 10 min ultrasonic bath; 7% sodium pyrophosphate ($Na_2P_2O_7$) solution was added to the solution to separate clay particles. All samples were centrifuged (at 3500 rpm for 13 min) to separate the supernatant, and cleaned thoroughly with deionised water.

A Malvern Mastersizer 2000 laser diffraction analyser was used to measure particle-size distributions (PSDs). The average of four analyses per sample was used. Grain-size statistics (Folk and Ward, 1957) were calculated using GRADISTAT (Blott and Pye, 2001).

Second, bulk sediments were placed in 10 cm^3 plastic pots and dried overnight in an oven at 42°C. Magnetic susceptibility of the samples was measured using a Bartington magnetic susceptibility MS2 meter and MS2B dual frequency sensor instrument. The background magnetic field was measured before and after each sample reading in order to control for natural drift in the Earth's magnetic field. Third, single grains were subsampled using 1% of sieved fractions (<32 μm, 63–125 μm, 125–250 μm, 250–500 μm, 500–1000 μm), mounted on glass slides with glycerine and visually counted. Grains were classified as glass shards if they presented at least three tephra-like morphological features: crossed-polar full extinction, the presence of bubble walls/cuspid shape, an absence of refraction, sharp edges and the absence of preferential crystallographic directions. Siliciclastic grains mainly comprised mica, quartz grains and undifferentiated clay mineral aggregates. Rare zircon and tourmaline were also present.

Results

Geochemistry

Table 1 shows the geochemical components of the Lenggong tephra. The fingerprints of the tephra samples confirm the nature and origin of the Lenggong unit as ejecta from the YTT eruption. The glass analyses of the samples from the Lenggong sites resemble those from the YTT reported in the literature (Fig. 3a). Minor differences between the new determinations and earlier data can be explained by the use of different standards for calibration, interlaboratory biases and the compatibility between analyses of individual glass shards versus bulk samples (cf. Acharyya and Basu, 1993; Shane et al., 1995; Pearce et al., 2008). Similarly, rare-earth element (REE) profiles of the Lenggong ash resemble the YTT REE profile reported in the literature (Fig. 3b). The results indicate relative enrichment in light REE, slight depletion of heavy REE and consistent, distinct negative Eu anomalies (Table 1, Fig. 3b).

Stratigraphy

All the samples investigated consist only of tephra, except for the siliciclastic units at the base of Kampung Luat 3. Kampung Luat 1 and 2 (5° 03.360′ N, 100° 58.864′ E, 68 m asl) occur on the opposite side of an artificial lake. Here the sandy tephra units (3.8 and 4.4 m thick, respectively) appear massive and show few or no sedimentological structures (Figs. 4a, b). No sharp changes in units and lithology were apparent.

The Kampung Luat 3 sequence (5° 03.833′ N, 100° 58.821′ E, 71 m asl) is 3.7 m thick in total, and consists of a lower, 1.19-m-thick siliciclastic unit (mainly clay and quartz), overlain by a 2.36-m-thick volcaniclastic sequence of sandy ash with horizontal laminations (Fig. 4c). The ash unit shows alternating light gray (10 YR 6/2–7/2) and gray (10 YR 5/1) laminations. The lower siliciclastic and the upper volcaniclastic sediments are divided by a ~20-cm-thick lens, composed of oxidised brownish yellow (10 YR 6/8) sandy ash, and delimited top and bottom by a 5–7 cm thick dark brown (7.5 YR 5/8) very finely wavy laminated reddish clay.

Table 1
Major and REE elements of the Lenggong ash. Standard deviations given in brackets.

wt%	Bukit Sapi	Kampung Luat 2	Kampung Luat 3
SiO_2	74.88 (1.16)	74.62 (1.13)	74.07 (1.16)
TiO_2	0.05 (0.05)	0.04 (0.05)	0.05 (0.05)
Al_2O_3	11.92 (0.29)	11.83 (0.32)	11.83 (0.29)
FeO	0.87 (0.34)	0.87 (0.32)	0.83 (0.34)
MnO	0.06 (0.08)	0.07 (0.08)	0.05 (0.08)
MgO	0.06 (0.06)	0.07 (0.05)	0.06 (0.05)
CaO	0.75 (0.09)	0.75 (0.12)	0.78 (0.09)
Na_2O	2.95 (0.19)	3.15 (0.22)	3.04 (0.20)
K_2O	5.13 (0.41)	5.03 (0.40)	5.07 (0.41)
n	31	32	18
Total	96.67	96.42	95.78
ppm	Bukit Sapi	Kampung Luat 2	Kampung Luat 3
La	18.09 (2.4)	21.38 (6.6)	24.73 (4.1)
Ce	37.76 (4.2)	49.37 (16.2)	50.21 (7.4)
Pr	3.55 (0.5)	4.641 (1.6)	4.7 (0.7)
Nd	12.56 (1.7)	16.85(6.0)	16.53 (3.0)
Sm	2.32 (0.4)	3.69(1.5)	3.42 (0.8)
Eu	0.28 (0.1)	0.29(0.1)	0.32 (0.1)
Gd	2.17 (0.6)	3.12(1.6)	2.98 (0.6)
Tb	0.39 (0.1)	0.63(0.3)	0.58 (0.2)
Dy	2.40 (0.3)	4.077(2.2)	3.67 (0.8)
Ho	0.53 (0.1)	0.95(0.5)	0.88(0.2)
Er	1.60 (0.4)	2.84(1.4)	2.55(0.6)
Tm	0.24 (0.01)	0.49(0.2)	0.44 (0.1)
Yb	2.13 (0.5)	3.88(1.9)	3.29(0.9)
Lu	0.31(0.1)	0.54 (0.2)	0.51 (0.1)
n	15	10	14

A fourth site, Bukit Sapi (BTS, 5° 08.776′N, 101° 01.398′E, 85 m asl) exposes a 3.7-m-thick sequence composed of a massive, light brownish gray (10 YR 4/2) silty and sandy ash (Fig. 4d). The ash outcrop can be visually subdivided into three ash 'sub-units' separated by sharp contacts: 1) basal silty ash with clay component, ~1 m thick, light brownish gray (10 YR 6/2); 2) upper sandy ash, 2.20 m thick, dark grayish brown (10 YR 4/2), covered by soil and vegetation in the top 30 cm; 3), block of massive, compacted fine ash, 50 cm thick, white (10 YR 8/1), sandwiched between sub-units 1) and 2); the block is ~1.5 m from the bottom of the section.

Sedimentology

Particle-size distributions for the Lenggong valley samples are provided in Table 2. Magnetic susceptibility (MS) and profile-averaged frequency distributions for each site are shown in Fig. 5.

The KgL1 YTT ash shows moderately sorted, unimodal grain-size distributions (Fig. 5a, Table 2). The particle-size distributions indicate a sand-dominated environment (64%), with a minor silt component (34%) and 2% clay. The mean grain-size values range between 57 and 100 μm (very coarse silt to very fine sand). The ash at KgL2 is poorly to very poorly sorted, mainly unimodal and bimodal (Fig. 5b, Table 2). The analyses indicate high variability through the vertical sequence, with no apparent grading. The sediment at KgL2 is composed of 62% sand, 37% silt and 1% clay, with means clustered at 100 μm (very fine sand, Table 2). The KgL3 sediments are polymodal, very poorly sorted and with substantial variations in mean particle sizes ranging from 51 to 178 μm (Fig. 5c, Table 2).

The BTS ash particle-size distributions range between 8 and 127 μm. The sediments at this site show a higher clay frequency within the lower part of the section (Fig. 5d), and in addition this is the only site where the silt component exceeds that of the sand (51% silt versus

https://doi.org/10.1016/j.yqres.2012.11.006 Published online by Cambridge University Press

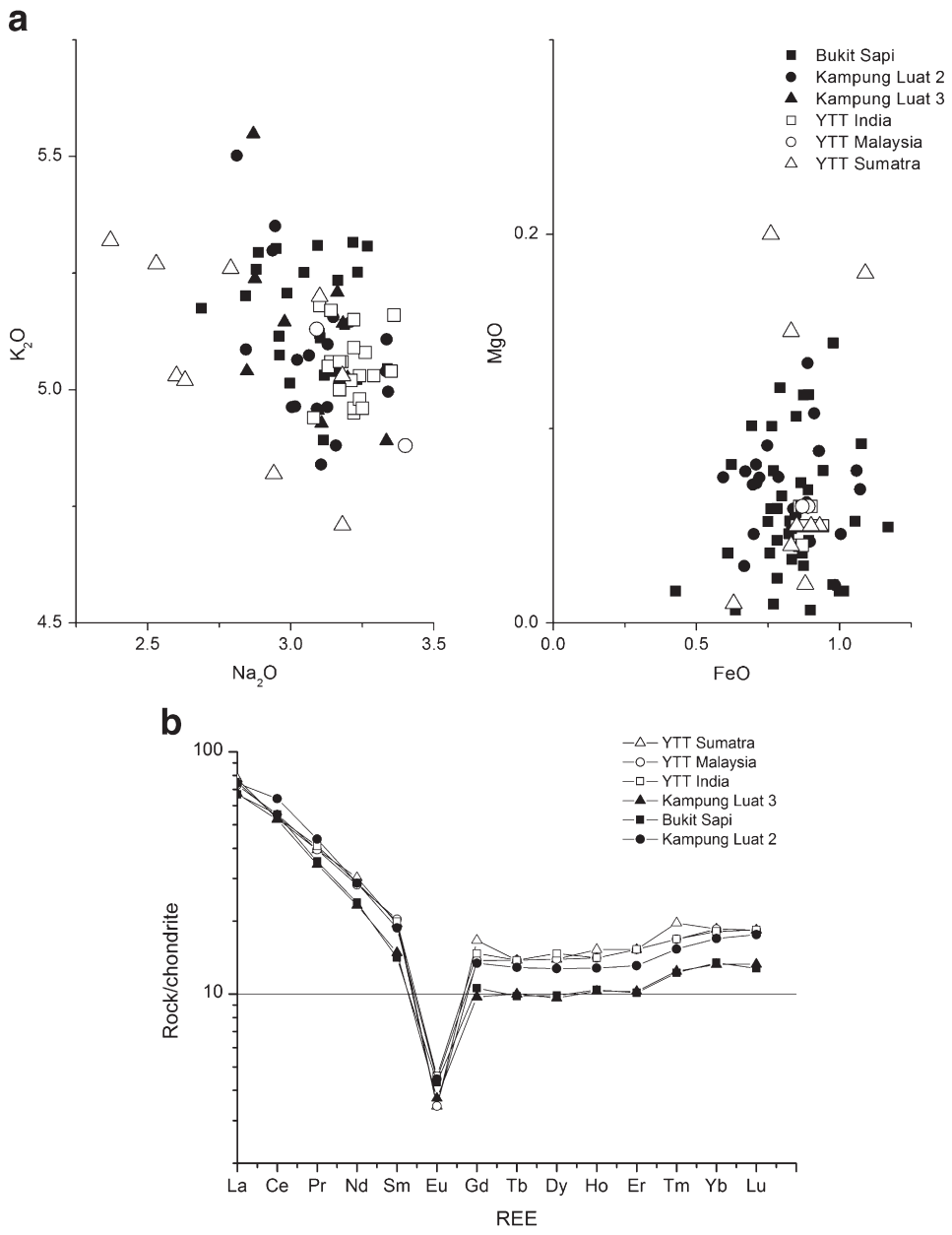

Figure 3. a) Major chemical components of the Lenggong ash compared with geochemical fingerprints of identified YTT glass from literature. Data from: Shane et al. (1995), Westgate et al. (1998), Smith et al. (2011) (India); Shane et al. (1995), Smith et al. (2011) (Malaysia); Westgate et al. (1998), Smith et al. (2011), Chesner (1998), Beddoe-Stephens et al. (1983) (Sumatra). It is noteworthy that the three proximal samples collected from the Toba caldera on Sumatra showed values differing slightly from those of distal areas. This could be explained by the sample type, indicated as welded tuff by the authors of the analyses. b) Rare earth element values for the YTT Lenggong valley ash and the literature references. Rare element analyses from Smith et al. (2011).

47% sand, Table 2). Standard deviations indicate poorly to very poorly sorted sediments, with trimodal frequency distributions in the lower part of the section but a unimodal distribution in the upper part.

The ash at BTS and KgL 2 is low in magnetic mineral content (Fig. 5). The samples from KgL3, as expected, show a stronger magnetic susceptibility of the oxidised lens (9.3×10^{-8} m^3 kg^{-1}), whereas KgL1 shows a weak magnetism at the level of the thin oxidised lens observed in sample KgL1-11 (6.4×10^{-8} m^3 kg^{-1}) but also a strong magnetism in sample KgL1-5 (22.6×10^{-8} m^3 kg^{-1}, Fig. 5, Table 2). All the samples reveal an increasing magnetic susceptibility towards the top, arising from contamination by overlying soils.

Taphonomic heterogeneity of the Lenggong deposits is reflected in their mineralogical associations. In the 63–125 μm interval, considered the dominant size interval for ash, the amount of ash ranges between 59 and 99%. In the >250 μm interval, considered the 'non-ash' fraction, the ash percentages range from 36% to 89% of the total. A few samples did not have substantial coarse fractions (indicated N/A in Table 3). The site that includes more ash is KgL1 (Table 3), which mineralogical components in the 63–125 μm fraction also show minor contents of quartz, zircon, tourmaline and mica. In contrast to KgL1, the KgL2 samples (particularly those from lower in the section), contain mica flakes, together with a minor quartz and zircon, representing 50 to 90% of the non-ash grains. Modern plant fragments have been identified in KgL2-9. The KgL3 ash is particularly variable: the proportion of ash in the sediments decreases sharply in the middle of the unit, before again increasing towards the top. As expected, the clay hardpans sandwiching the ash lens have low ash content (sample KgL3-12, Table 3).

https://doi.org/10.1016/j.yqres.2012.11.006 Published online by Cambridge University Press

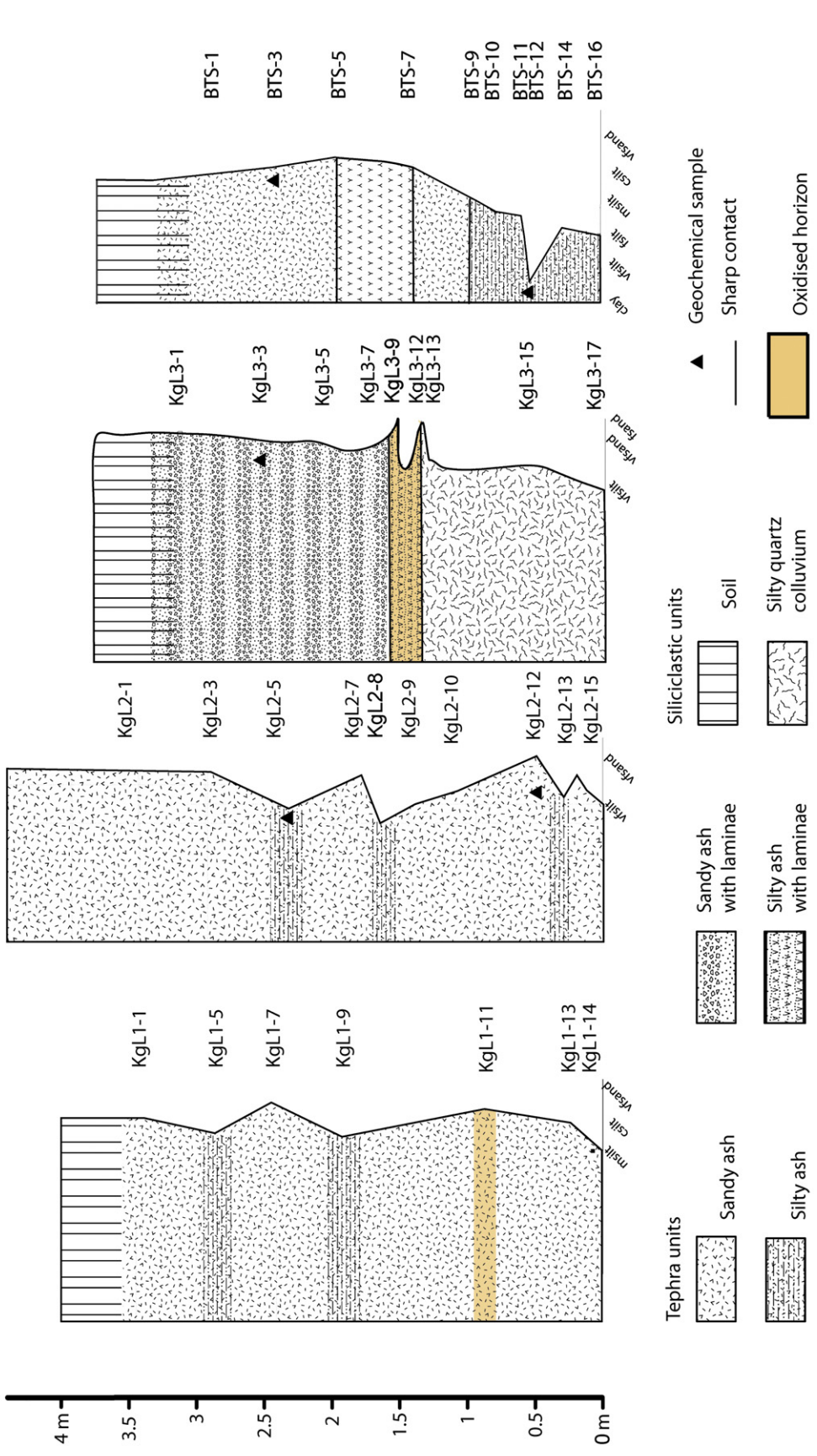

Figure 4. Schematic logs of the tephra sedimentary sequences. The tephra units are the main sedimentological components for all four sites. Five EMPA analyses have been obtained from the lower and upper units of KgL2, 3 and BTS, and, in conjunction with LA-ICPMS rare earth element analyses, confirmed the association of the tephra with the Youngest Toba Tuff.

https://doi.org/10.1016/j.yqres.2012.11.006 Published online by Cambridge University Press

Table 2
Selected particle size distribution parameters for the Lenggong valley YTT ash. Grain-size distributions measured on Malvern Mastersizer 2000, data quoted as average of 4 analyses per sample. Mean particle size quoted as geometric mean following methodology of Blott and Pye (2001). Particle fractions are chosen based on ash grain-size classification divisions.

Sample ID	Mean (μm)	Sorting (μm)	63–125 μm fraction of the total	>250 μm fraction of the total	Distribution	Sorting
KgL3-1	115.9	3.6	29%	28%	Bimodal	Poorly sorted
KgL3-3	93.13	2.9	47%	14%	Unimodal	Poorly sorted
KgL3-5	89.64	5.2	28%	29%	Trimodal	Very poorly sorted
KgL3-7	77.17	3.5	40%	15%	Unimodal	Poorly sorted
KgL3-8	178.7	4.2	28%	29%	Bimodal	Very poorly sorted
KgL3-9	51.04	3.3	49%	6%	Bimodal	Poorly sorted
KgL3-11	151.9	2.9	27%	34%	Bimodal	Poorly sorted
KgL3-12	123.8	5.4	24%	35%	Trimodal	Very poorly sorted
KgL3-13	52.68	4.5	38%	12%	Trimodal	Very poorly sorted
KgL3-15	59.17	5.0	29%	17%	Trimodal	Very poorly sorted
KgL3-17	33.21	4.1	45%	4%	Trimodal	Very poorly sorted
KgL2-1	121.2	4.8	25%	37%	Trimodal	Very poorly sorted
KgL2-3	110.9	4.3	24%	33%	Unimodal	Very poorly sorted
KgL2-5	59.35	5.2	27%	24%	Bimodal	Very poorly sorted
KgL2-7	111.3	3.9	27%	30%	Bimodal	Poorly sorted
KgL2-8	46.96	2.4	65%	0	Unimodal	Poorly sorted
KgL2-9	65.01	3.7	39%	11%	Unimodal	Poorly sorted
KgL2-10	81.75	3.9	35%	20%	Bimodal	Poorly sorted
KgL2-12	155.0	4.2	21%	46%	Unimodal	Very poorly sorted
KgL2-13	74.36	4.1	37%	19%	Bimodal	Very poorly sorted
KgL2-14	116.5	3.7	29%	30%	Bimodal	Poorly sorted
KgL2-15	78.29	4.5	31%	22%	Bimodal	Very poorly sorted
KgL1-1	83.21	4.3	30%	21%	Unimodal	Very poorly sorted
KgL1-3	71.92	3.5	44%	12%	Unimodal	Poorly sorted
KgL1-5	100.5	3.3	34%	20%	Unimodal	Poorly sorted
KgL1-7	68.51	3.5	44%	10%	Bimodal	Poorly sorted
KgL1-11	95.21	3.7	32%	22%	Unimodal	Poorly sorted
KgL1-13	78.52	3.3	41%	12%	Unimodal	Poorly sorted
KgL1-14	57.55	3.1	53%	5%	Unimodal	Poorly sorted
BTS-1	86.15	2.8	45%	5%	Unimodal	Poorly sorted
BTS-3	109.2	2.6	40%	17%	Unimodal	Poorly Sorted
BTS	127.5	2.5	35%	20%	Unimodal	Poorly sorted
BTS-7	111.1	3.2	33%	20%	Bimodal	Poorly sorted
BTS-9	54.72	2.5	69%	0%	Unimodal	Poorly sorted
BTS-10	41.27	2.5	67%	0%	Unimodal	Poorly sorted
BTS-11	36.56	6.9	17%	19%	Polymodal	Very poorly sorted
BTS-12	8.233	4.8	6%	1%	Bimodal	Very poorly sorted
BTS-14	28.84	5.9	13%	15%	Trimodal	Very poorly sorted
BTS-16	23.88	3.9	29%	7%	Bimodal	Poorly sorted

Discussion

The tephra units of the Lenggong valley are geochemically similar to those reported as YTT from other sites (Shane et al., 1995; Westgate et al., 1998; Petraglia et al., 2007; Smith et al., 2011). Since the Lenggong ash was derived from the same eruption, and assuming it was deposited contemporaneously, any differences between the sites (i.e., thickness, mineralogy, grain size) should reflect post-deposition processes.

Primary and reworked tephra: a reliable method of distinction?

The exposed tephra deposits in the Lenggong valley present general taphonomic characteristics that reveal the reworked nature of the sediments: they are up to ~4 m in thickness, include structures such as wavy laminations and have non-volcanic components that imply mixing with other sedimentary detritus prior to final deposition. No primary ash was found at the sites.

A recent study of the primary ash layer in the Son Valley, India, showed a distinctive difference between the primary ash particle-size distributions—described as well sorted, unimodal, with mean centred between 63 and 50 μm—and the reworked ash deposits above the primary stratum, characterized by polymodal distributions, poor sorting and the presence of coarser particles (Lewis et al., 2012). Figure 6 shows a comparison between the particle-size distributions from Jwalapuram site 3 (Jones, 2010), and site KgL1. Jwalapuram exposes 5 cm of primary ash and 2.30 m of overlying reworked material. The plot shows that particle-size distributions of both the primary and reworked material from India and Malaysia are similar. The KgL1 samples are skewed towards the right (very fine skewness), compared with the Indian ash samples. However, all the Indian tephra show a similar skewness, independent of their being primary or reworked. Skewness may therefore develop through plume dispersion in the atmosphere, rather than provide a diagnostic of primary ash.

Furthermore, the presence of coarser particles should not be taken as an indication of non-volcanic particles (and thus an indication of reworking). Scanning electron microscope images of grains from sample KgL2-1 reveal that the larger grain-size fraction is composed of ash aggregates and not non-volcanic grains (Fig. 7). Ash particle aggregation is a widely recognized phenomenon in distal tephra deposits, although the process remains only partially understood. It could occur either during atmospheric transport or post-depositionally (Folch et al., 2010).

In summary, if the primary facies can be seen in the field, features such as moderate sorting, unimodality and high ash content can reliably be applied to support the interpretation (Table 4). However, these features cannot exclude the possibility that the ash is reworked: since as shown, secondary ash can be well sorted, fine and unimodal. This implies that where there is not a clearly exposed outcrop (for example in the case of microtephra in caves or cryptotephra in lake cores), such techniques cannot be considered sufficiently robust to discriminate between the two (cf. Davies et al., 2007; Morley and Woodward, 2011).

The Kota Tampan YTT layer and archaeological implications

Collings (1938, p. 575) described the ash at Kota Tampan as a "deposit of volcanic tuff overlying a bed of sand and gravel, which

https://doi.org/10.1016/j.yqres.2012.11.006 Published online by Cambridge University Press

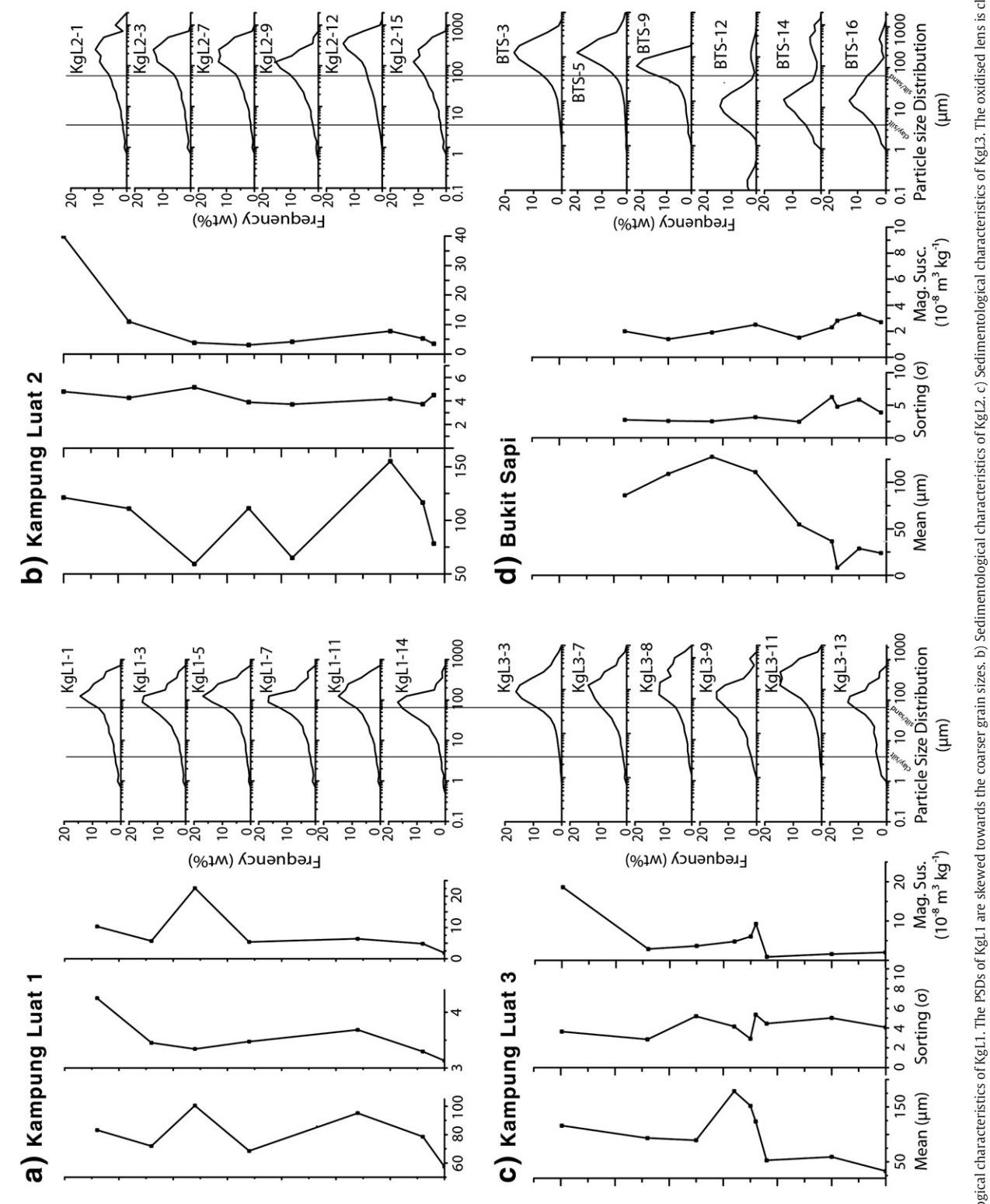

Figure 5. a) Sedimentological characteristics of KgL1. The PSDs of KgL1 are skewed towards the coarser grain sizes. b) Sedimentological characteristics of KgL2. c) Sedimentological characteristics of KgL3. The oxidised lens is clearly evident in the MS of profile. High MS values towards the top units are probably sign of contamination by the upper soil. d) Sedimentological characteristics of BTS. BTS presents the finer grain size, with a 2% of clay and 51% silt. This is visible in the particle size distribution, shifted towards finer grain size. It is also in accordance with the geomorphic reconstruction of the site, which indicated BTS does not belong to the same depositional environment of KgLs but to a small tributary.

https://doi.org/10.1016/j.yqres.2012.11.006 Published online by Cambridge University Press

Table 3
Ash content by mass in the Lenggong valley tephra deposits.

Site	63–125 μm Ash fraction	>250 μm Ash fraction
KgL1-1	88%	75%
KgL1-3	96%	71%
Kgl1-5	92%	86%
KgL1-7	96%	N/A
KgL1-11	94%	89%
KgL1-13	95%	N/A
KgL1-14	99%	N/A
KgL2-1	70.61%	85%
KgL2-3	76.74%	87%
KgL2-5	83.64%	71%
KgL2-8	77.18%	N/A
KgL2-9	89.27%	36%
KgL2-12	76.73%	69%
KgL2-15	74.37%	78%
KgL3-1	91%	98%
KgL3-3	93%	48%
KgL3-5	59%	61%
KgL3-7	78%	58%
KgL3-8	93%	49%
KgL3-11	92%	84%
KgL3-12	22%	10%

itself rests on laterite, […] probably an old terrace of the Perak River". The ash was reported to be 3 m in thickness, overlying gravel beds from which Palaeolithic implements belonging to 'Tampanian' industry had been recovered (Collings, 1938). Although the ash was not then characterized as primary or secondary, this author's stratigraphical description appears comparable to that at KgL3. Stauffer (1973) obtained a date of ~35 ka for the Tampan tools, based on ^{14}C dating of wood obtained immediately underlying the ash. Later the dating of the YTT ash to 75 ka led to a corresponding increase in the age of the Tampanian tools (Ninkovich et al., 1978). However, by comparison with the sequences examined here, the excessive thickness of the Kota Tampan ash provides a strong suggestion of the secondary nature of the deposit. Since there is no record of a basal primary ash unit at this site, the implication is that the Kota Tampan ash could be reworked and deposited at a later date. This implies that the Kota Tampan YTT marker cannot guarantee that the tools below the ash are older or contemporaneous with the YTT.

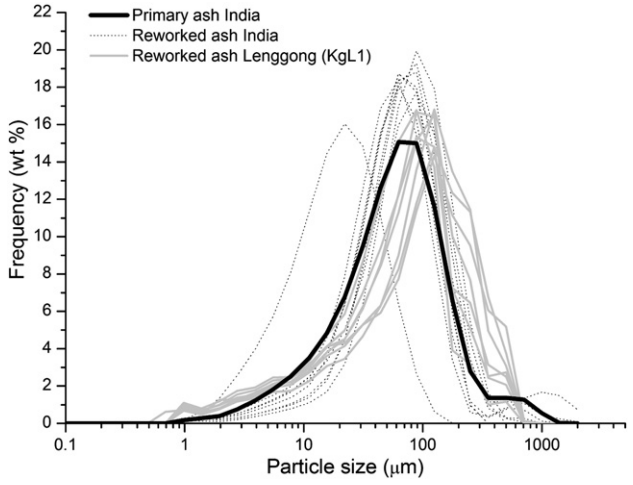

Figure 6. Particle-size distributions for the primary ash found at Jwalapuram site 3 and the reworked tephra from the Lenggong valley. The particle-size distributions from the Indian and Malaysian samples are similar. The primary ash sample (in bold) is symmetric and has a finer mean peak compared to the Malaysian reworked tephra. However, ash aggregation could account for such a discrepancy. Primary ash data from Jones (2010).

Mechanism of tephra reworking in the Lenggong valley

The reported sedimentary structures and the particle-size distributions consistently suggest fluvial transport as the main process of accumulation and deposition of the distal tephra in the Lenggong valley. The absence of grading argues against tephra fallout as the predominant depositional process. All the sequences studied are poorly to very poorly sorted, classified texturally as muddy sand, and sedimentologically classified as coarse silt, very coarse silt or very fine sand (Table 2). The deposits of Kgl1, KgL2 and BTS are massive, while KgL3 showed horizontal laminations and planar bedding. Modern plant material has been found in all the deposits, particularly in KgL2. The percentage of ash varies in each deposit, although the principal grain-size interval (63–125 μm) contains 71–99% ash.

The tephra at KgL3, situated near the main channel, includes marked horizontal laminae and an oxidised ash lens ~10 cm thick, sandwiched between two ~5-cm-thick clay hardpans. The lens is capped by 2.30 m of reworked tephra, sub-horizontally parallel laminated. The basal contact with the non-volcanic unit is non-erosional. The upper deposits at KgL3 are the product of the transport and redisposition of ash remobilised from upstream, probably by a flood flow. Yet the wavy, laminated clay hardpans indicate deposition from suspension in slack water, and the oxidized lens sandwiched within the hardpans suggests that the deposit was temporarily exposed to air, before being flooded and buried by more ash. We suggest that KgL3 was deposited in a vegetated floodplain or swamp, characterized by seasonal flooding and desiccation (Nakayama and Yoshikawa (1997). Similar tephra deposits separated by clay hardpans have been identified at Jwalapuram, in India (Petraglia et al., 2007). The deposit shows six clay hardpans through the ash sequence. Petraglia et al. (2007) interpreted the couplets as representing six monsoon cycles, characterized by wet (ash) and dry (clay) periods. KgL3 includes two clay hardpans, suggesting that the lens might represent one rainy season embedded between two dry seasons.

The ash at KgL1 and 2 was deposited in a depression. The particle-size distributions and mineralogical associations indicate a chaotic mixture of silty-sized ash and fine-sand-sized ash. This suggests that the two sequences are likely to be derived from slumping sedimentation in a colluvial area (Kataoka, 2005), possibly during a major flood event that remobilised the fall deposits from the surrounding hills. Kataoka (2005) interpreted such volcaniclastic facies as a direct effect of the low liquefaction resistance of volcaniclastic deposits (Nakayama, 2001). Such types of slump deposits have been identified in volcaniclastic sequences in the Pliocene Mushono tephra, in central Japan (Kataoka, 2003, 2005).

We note that, although KgL1 and 2 are likely to have been deposited during the same slumping event, they show contrasting sedimentological characteristics. The high mica content at KgL2 (Fig. 5b) could have arisen from site-specific syn- or post-depositional processes. The bedrock underlying the catchment is micaceous granite. A nearby tributary could therefore have brought allochthonous mica from its local catchment. Alternatively, the KgL2 ash might originally have been closer to the paleo-channel bank, where it could have been more exposed to local bedrock weathering. At this site the lower units appear to be enriched in mica, probably eroded from underlying granites during flood events. Conversely the mica could also be a primary magmatic component of the YTT tephra, since biotite is a primary product of the YTT eruption (Chesner, 1998; Smith et al., 2011), and the accumulation of mica flakes in the basal stratum could be related to the density differences between mica ($\rho = 2900$ kg/m^3) and rhyolite glass shards ($\rho = 2350$–2450 kg/m^3). However, mica flakes may behave very differently from glass shards hydrodynamically, and the shape of the grains could potentially be more important than density. This suggests that several site-specific parameters determined the final characteristics of the preserved deposits.

https://doi.org/10.1016/j.yqres.2012.11.006 Published online by Cambridge University Press

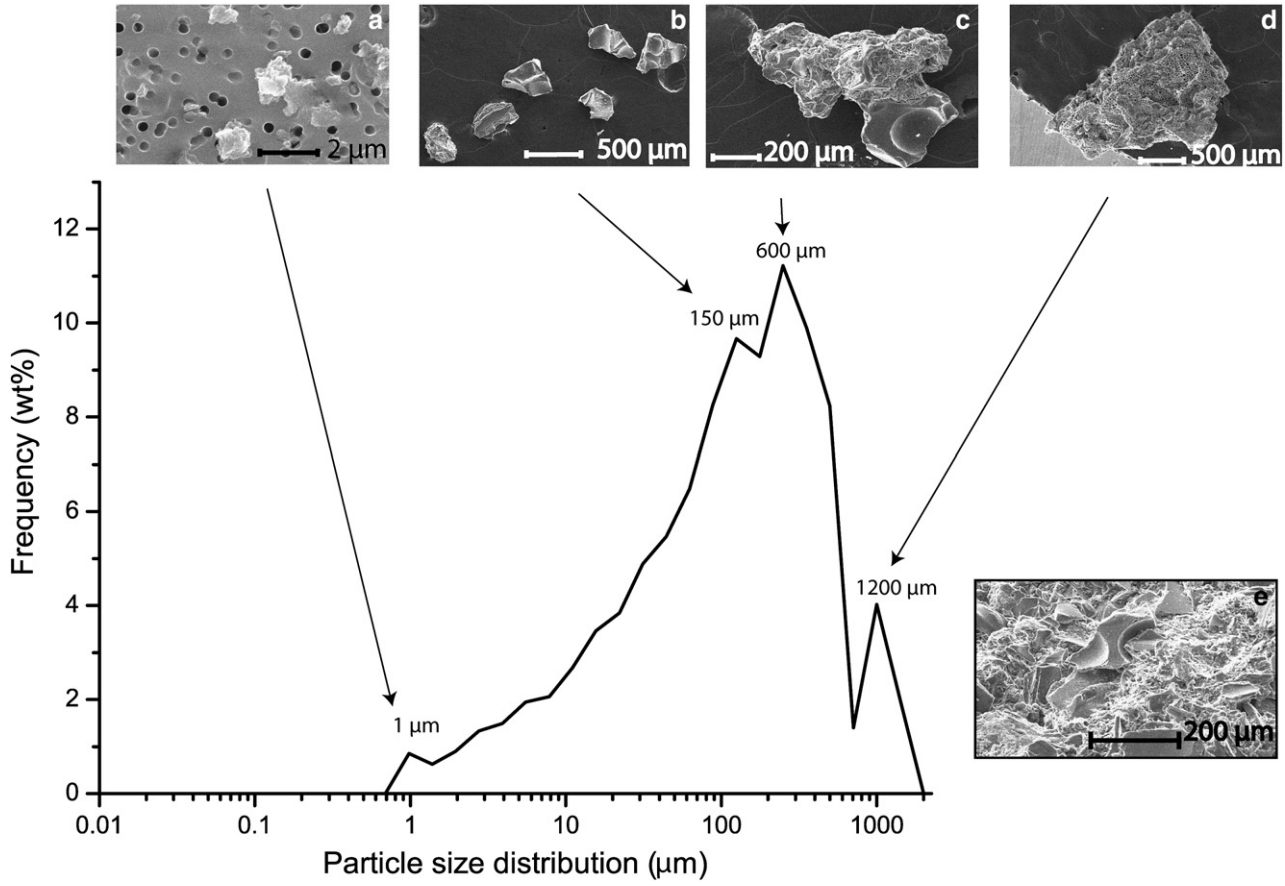

Figure 7. Polymodality is a typical characteristic of distal tephra horizons, arising from the poor sorting and ash aggregations. Polymodality and unimodality are thus not diagnostic features to distinguish between primary and secondary ash. It is notable that two of three peaks in sample KgL2-1 are composed of ash shards (b) and ash shard aggregates (c, d). Photo e shows a zoom on a 1200-µm aggregate: it is possible to distinguish the cemented silica matrix and the micro glass fragments.

Further work is required to understand the presence of mica in the KgL2 unit.

BTS is massive in aspect, similar to KgL2 1 and 2. However, the textural analyses showed that BTS is consistently finer (2% clay) and presents clear alternating subunits of clay-like and silty ash (Figs. 4, 5). The magnetic susceptibility reveals clear differences between the lower and the upper silt (Fig. 5). Massive resedimented units indicate that reworking occurred through hyperconcentrated flows, resulting in sudden aggradation of ash (Kataoka, 2005; Manville et al., 2005). We thus suggest that BTS is the result of a mudflow (Nakayama and Yoshikawa, 1997), and the changes in particle size between the bottom and the top could indicate waxing and waning flow. Examples of similar lahar facies have been reported for the Ebisutoge–Fukuda tephra (Kataoka et al., 2009), and Ohta tephra of the Tokai Group (Nakayama and Yoshikawa, 1997), both in central Japan.

Time of deposition and implications for the YTT environmental impact

Magnetic susceptibility of sediments is an indicator of soil-forming processes in areas containing uniform parent material (Mullins, 1977). The constant values recorded by the samples analysed suggest the tephra accumulated in a short period of time. Neither the sedimentation rate, nor the total accumulation time for each deposit can be determined in the absence of bracketing ages below and above the units, and such data

Table 4
General characteristics of primary and secondary ash units. The combination of these features can usually distinguish between primary and secondary ash in terrestrial distal deposits where the tephra appear in meter-thick outcrops. The problems occur when the ash is found in sub-millimetre-scale strata, i.e. in cryptotephra or microtephra.

	Primary ash	Secondary ash
Thickness	Cm-scale (usually 4–10 cm)	Can reach 10+ m
Color	White looking (10 YR 8/1 and 8/2; 7.5 YR 8/2)	Wide range of gray-toned colours (10 YR 4/2; 10 YR 8/3, 7/3 and 7/4)
Basal contact	Sharp non-erosive	Gradual; erosive; non-erosive
Upper contact	Sharp non-erosive if sealed by non-volcanic sediments (usually marine/lacustrine environment); gradual if overloaded by reworked units/bioturbated	Gradual; erosive; non-erosive
Sedimentary structures	Variable, but usually no traces of vertical grading and water percolation structures; ball and pillow structures can be found at the upper boundary, if the ash was deposited in an aqueous environment	Variable: massive, horizontal stratification, ripple-cross lamination, parallel thin lamination, cross-bedded.
Grain shape	No difference	No difference
Grain-size distributions	Unimodal	Unimodal; polymodal
Lateral persistency	Very variable	Consistent; variable
Cementation	Variable	Variable

https://doi.org/10.1016/j.yqres.2012.11.006 Published online by Cambridge University Press

are not available for the time being for the Lenggong deposits (neither volcanic nor siliciclastic). Nevertheless, the facies suggest mudflow, slumping and flood flow as the main depositional processes, mechanisms that usually operate on time scales of hours to days (Mastrolorenzo et al., 2002). Given the monsoonal climate operating in the region and the associated high rainfall intensities, the tephra was probably emplaced within few years from the initial eruption. This is supported by the mineralogical data showing a relative high purity of the reworked ash. The only site that suggests subaerial exposure and a clear depositional hiatus is KgL3. Here a lens of ~10 cm of ash was deposited, probably from material in suspension, and sealed between two clay hardpans. This site is therefore the best candidate for potential paleoenvironmental studies in the area.

Nevertheless, attention is required when interpreting the paleoenvironmental signals extracted from reworked tephra. Although the ash probably emplaced shortly after the eruption, the precise time lag between the primary deposition of the YTT and the flood events is unknown. Therefore, the correlation between paleo-records and the environmental impact of the ashfall can only be roughly inferred. Furthermore, the records are likely to be influenced by site-specific morphological characteristics. This has been recently considered by Blinkhorn et al. (2012). These authors demonstrated that the oxygen and carbon stable isotope traces extracted from pedogenic carbonate beneath and overlying the YTT in twelve terrestrial deposits at Jwalapuram were extremely variable. Such variability appeared directly linked to site-specific features (i.e., topographic height), rather than post-eruptive environmental feedbacks. This recent discovery reinforces our results demonstrating the strong controls of the receiving environments on the tephra taphonomy. These have profound implications for the wider YTT debate, where conclusions regarding a drastic impact of the ashfall have been reached based on paleo-environmental reconstructions from proxies extracted from reworked tephra sequences (e.g., Williams et al., 2009; Haslam et al., 2010). In the light of the process highlighted herein, such conclusions may be unsafe. In a broader sense the processes identified indicate that environmental techniques must be adapted to reflect the sedimentological and stratigraphical characteristics of the tephra sediments at any particular site.

Conclusions

Analysis of the stratigraphy and sedimentology of four new YTT localities in the Lenggong valley, Malaysia has demonstrated that these tephra sequences are associated with fluvial and colluvial transport and deposition. Three volcaniclastic facies have been identified corresponding to flood-flow, mudflow and slumping sedimentation. Both major elements and REE chemical fingerprints confirm that the tephra in these facies corresponds to the YTT eruption (~73 ka).

The field stratigraphy, particle mineralogical associations and size distribution of the sediments together indicate that the tephra deposits are reworked. The data suggest that the ash deposition occurred rapidly, on the scale of days or months. Although there are no dates currently available for the Lenggong sediments, further studies should be undertaken in order to assess the absolute age of the flood events and their accumulation rate. KgL3 is the only site where non-volcanic material is exposed beneath the ash and where the mechanism of deposition allowed the development of an undisturbed ash unit. It should therefore be a good target for further studies to establish the detailed depositional chronology. The investigations reported here suggest that other areas of Peninsular Malaysia are likely to host YTT deposits. These include the Singar sub-catchment and the Temengor Lake, which potentially provide a test for the mechanisms of accumulation and preservation outlined here.

Analyses of the mechanism of tephra reworking are particularly important in the case of the YTT, given the wide use of the ash deposits in distal areas to assess the YTT environmental impact and its possible consequences for human populations. The results highlight the need to address new questions to refine the YTT debate; for example: how can the rate of accumulation of the reworked ash sequence be determined? Are there paleoenvironmental proxies that can be extrapolated from the reworked sequence and undoubtedly related to the ashfall impact?

On a global scale, the work reported herein demonstrates the importance of producing a detailed examination of tephra units and their sedimentary environments, particularly when the tephra units are used for chronological correlation, and where the occurrence of the ashfall could have had strong environmental impacts. This is particularly important in situations where substantial sediment transport and topographic contrasts predominate, such as in Malaysia.

A major problem in the application of tephra for chronology and stratigraphy is the differentiation between primary and secondary ash. We have demonstrated that particle-size analyses alone cannot be used in isolation to distinguish between the two. This has significant implications when correlation is based on micro-tephra or cryptotephra. A new method is therefore required to differentiate unequivocally between the primary and secondary ash facies. Ideally this should be a micro-scale technique that allows differentiation between the two on the basis of the characteristic features of single grains. Such an approach could include, for example, lithogenic radioactive isotopes extracted from the non-volcanic material within the ash, or diagenetic processes occurring on the ash surface (e.g., Kuznetsova et al., 2009).

Acknowledgments

E.G. gratefully acknowledges fieldwork support from the Royal Geographical Society (Dudley Stamp Memorial Award), the SMUTS Memorial Fund and the Philip Lake Fund (University of Cambridge). Laboratory analyses were funded through awards from Sidney Sussex College, the Department of Geography of the University of Cambridge, and the William George Fearnsides Fund (Geological Society of London). We thank Stephen Oppenheimer for facilitating the contact with Prof. Mokthar, Mr. Aznar (Universiti Sains Malaysia) for kind assistance with fieldwork, and Steve Boreham, Chris Rolfe, Chiara Petrone and Jason Day for laboratory support. E.G. particularly thanks Mike Morley, Steve Boreham, Keith Richards and Adam Durant for discussions and comments on the manuscript. We are grateful to J. Westgate, M. Williams, D. Booth and J. O'Connor for valuable comments on the original manuscript.

References

Acharyya, S.K., Basu, P.K., 1993. Toba ash on the Indian subcontinent and its implications for correlation of Late Pleistocene alluvium. Quaternary Research 40 (1), 10–19.
Alloway, B.V., Larsen, G., Lowe, D.J., Shane, P.A.R., Westgate, J.A., 2007. In: Scott, A.E. (Ed.), Quaternary Stratigraphy | Tephrochronology, Encyclopedia of Quaternary Science. Elsevier, Oxford, pp. 2869–2898.
Ambrose, S.H., 1998. Late Pleistocene human population bottlenecks, volcanic winter, and differentiation of modern humans. Journal of Human Evolution 34 (6), 623–651.
Ambrose, S.H., 2003. Did the super-eruption of Toba cause a human population bottleneck? Reply to Gathorne-Hardy and Harcourt-Smith. Journal of Human Evolution 45 (3), 231.
Beddoe-Stephens, B., Aspden, J.A., Shepherd, T.J., 1983. Glass inclusions and melt compositions of the Toba Tuffs, northern Sumatra. Contributions to Mineralogy and Petrology 83 (3), 278–287.
Blinkhorn, J., Parker, A.G., Ditchfield, P., Haslam, M., Petraglia, M., 2012. Uncovering a landscape buried by the super-eruption of Toba, 74,000 years ago: a multi-proxy environmental reconstruction of landscape heterogeneity in the Jurreru Valley, south India. Quaternary International 258, 135–147.
Blott, S.J., Pye, K., 2001. GRADISTAT: a grain size distribution and statistics package for the analysis of unconsolidated sediments. Earth Surface Processes and Landforms 26 (11), 1237–1248.
Chesner, C.A., 1998. Petrogenesis of the Toba Tuffs, Sumatra, Indonesia. Journal of Petrology 39 (3), 397–438.
Chesner, C.A., Rose, W.I., 1991. Stratigraphy of the Toba-Tuffs and the evolution of the Toba-Caldera Complex, Sumatra, Indonesia. Bulletin of Volcanology 53 (5), 343–356.
Chesner, C.A., Rose, W.I., Deino, A., Drake, R., Westgate, J.A., 1991. Eruptive history of Earth's largest Quaternary caldera (Toba, Indonesia) clarified. Geology 19 (3), 200–203.
Collings, H.D., 1938. Pleistocene site in the Malay Peninsula. Nature 3595, 575–576.

https://doi.org/10.1016/j.yqres.2012.11.006 Published online by Cambridge University Press

Davies, S.M., Elmquist, M., Bergman, J., Wohlfarth, B., Hammarlund, D., 2007. Cryptotephra sedimentation processes within two lacustrine sequences from west central Sweden. The Holocene 17 (3), 319–330.
Davies, S.M., Abbott, P.M., Pearce, N.J.G., Wastegård, S., Blockley, S.P.E., 2012. Integrating the INTIMATE records using tephrochronology: rising to the challenge. Quaternary Science Reviews 36, 11–27.
Folch, A., Costa, A., Durant, A., Macedonio, G., 2010. A model for wet aggregation of ash particles in volcanic plumes and clouds: 2. Model application. Journal of Geophysical Research 115 (B9), B09202.
Folk, R.L., Ward, W.C., 1957. Brazos River bar [Texas]; a study in the significance of grain size parameters. Journal of Sedimentary Research 27 (1), 3–26.
Gathorne-Hardy, F.J., Harcourt-Smith, W.E.H., 2003. The super-eruption of Toba, did it cause a human bottleneck? Journal of Human Evolution 45 (3), 227–230.
Gatti, E., Oppenheimer, C., 2012. Utilization of distal tephra records for understanding climatic and environmental consequences of the Youngest Toba Tuff. In: Giosan, L., Fuller, D., Nicoll, R., Flad, R.K., Clift, P.D. (Eds.), Climates, Landscapes and Civilizations, Geophys. Monogr. Ser., vol. 198, pp. 63–74 AGU, Washington, DC.
Gatti, E., Durant, A.J., Gibbard, P.L., Oppenheimer, C., 2011. Youngest Toba Tuff in the Son Valley, India: a weak and discontinuous stratigraphic marker. Quaternary Science Reviews 30 (27–28), 3925–3934.
Haslam, M., Petraglia, M., 2010. Comment on "Environmental impact of the 73 ka Toba super-eruption in South Asia" by M.A.J. Williams, S.H. Ambrose, S. van der Kaars, C. Ruehlemann, U. Chattopadhyaya, J. Pal and P.R. Chauhan [Palaeogeography, Palaeoclimatology, Palaeoecology 284 (2009) 295–314]. Palaeogeography, Palaeoclimatology, Palaeoecology 296 (1–2), 199–203.
Haslam, M., Clarkson, C., Petraglia, M., Korisettar, R., Jones, S., Shipton, C., Ditchfield, P., Ambrose, S.H., 2010. The 74 ka Toba super-eruption and southern Indian hominins: archaeology, lithic technology and environments at Jwalapuram Locality 3. Journal of Archaeological Science 37 (12), 3370–3384.
Jones, S.C., 2010. Palaeoenvironmental response to the 74 ka Toba ash-fall in the Jurreru and Middle Son valleys in southern and north-central India. Quaternary Research 73 (2), 336–350.
Jones, S.C., 2012. Local- and regional-scale impacts of the 74 ka Toba supervolcanic eruption on hominin populations and habitats in India. Quaternary International 258, 100–118.
Jones, S.C., Pal, J.N., 2009. The Palaeolithic of the Middle Son valley, north-central India: changes in hominin lithic technology and behaviour during the Upper Pleistocene. Journal of Anthropological Archaeology 28 (3), 323.
Kale, V.S., Patil, D.N., Powar, N.J., Rajaguru, S.N., 1993. Discovery of a volcanic ash bed in the alluvial sediments at Morgaon, Maharashtra. Man and Environment 18, 141–143.
Kataoka, K., 2003. Volcaniclastic remobilization and resedimentation in distal terrestrial settings in response to large-volume rhylitic eruptions: examples from the Plio-Pleistocene volcaniclastic sediments, central Japan. Journal of Geosciences (46), 47–65.
Kataoka, K., 2005. Distal fluvio-lacustrine volcaniclastic resedimentation in response to an explosive silicic eruption: the Pliocene Mushono tephra bed, central Japan. Geological Society of America Bulletin 117 (1–2), 3–17.
Kataoka, K.S., Manville, V., Nakajo, T., Urabe, A., 2009. Impacts of explosive volcanism on distal alluvial sedimentation: examples from the Pliocene–Holocene volcaniclastic successions of Japan. Sedimentary Geology 220 (3–4), 306.
Korisettar, R., Mishra, S., Rajaguru, S.N., Gogte, V.D., Ganjoo, r.K., Venkatesan, T.R., Tandon,, s.K., Somayajulu, B.L.K., Kale, V.S., 1988. Age of the Bori volcanic ash and Lower Palaeolithic culture of the Kukdi Valley, Maharashtra. Bulletin of the Deccan College Postgraduate and Research Institute 48, 135–138.
Kuznetsova, E.P., Motenko, R.G., Vigasina, M.F., Mel'chakova, L.V., 2009. IR spectroscopy and thermal study of volcanic ashes of different age: annual seminar on experimental mineralogy, petrology and geochemistry. Bulletin of Environmental Sciences RAS 1 (27), 83.
Lewis, L., Ditchfield, P., Pal, J.N., Petraglia, M., 2012. Grain size distribution analysis of sediments containing Younger Toba tephra from Ghoghara, Middle Son valley, India. Quaternary International 258, 180–190.
Lowe, D.J., 2011. Tephrochronology and its application: a review. Quaternary Geochronology 6 (2), 107–153.
Lowe, J.J., Walker, M.J.C., 1984. Reconstructing Quaternary Environments. Longman Scientific and Technical, London.
Manville, V., Newton, E.H., White, J.D.L., 2005. Fluvial responses to volcanism: resedimentation of the 1800a Taupo ignimbrite eruption in the Rangitaiki River catchment, North Island, New Zealand. Geomorphology 65 (1–2), 49–70.
Margari, V., Pyle, D.M., Bryant, C., Gibbard, P.L., 2007. Mediterranean tephra stratigraphy revisited: results from a long terrestrial sequence on Lesvos Island, Greece. Journal of Volcanology and Geothermal Research 163 (1–4), 34.
Mason, B.G., Pyle, D.M., Oppenheimer, C., 2004. The size and frequency of the largest explosive eruptions on Earth. Bulletin of Volcanology 66 (8), 735–748.
Mastrolorenzo, G., Palladino, D.M., Vecchio, G., Taddeucci, J., 2002. The 472 AD Pollena eruption of Somma-Vesuvius (Italy) and its environmental impact at the end of the Roman Empire. Journal of Volcanology and Geothermal Research 113 (1–2), 19–36.
Matthews, N.E., Smith, V.C., Costa, A., Durant, A.J., Pyle, D.M., Pearce, N.J.G., 2012. Ultra-distal tephra deposits from super-eruptions: examples from Toba and New Zealand. Quaternary International 258, 54–79.
Mokhtar, S., 2009. Debu Gunung Berapi di Lembah Lenggong, Perak. Journal Arkeologi Malaysia 22, 1–12.
Morgan, R.P.C., 1973. The influence of scale in climatic geomorphology: a case study of drainage density in West Malaysia. Geografiska Annaler Series A, Physical Geography 55 (2), 107–115.
Morley, M.W., Woodward, J.C., 2011. The Campanian Ignimbrite (Y5) tephra at Crvena Stijena Rockshelter, Montenegro. Quaternary Research 75 (3), 683–696.
Mullins, C.E., 1977. Magnetic susceptibility of the soil and its significance in soil science—a review. Journal of Soil Science 28 (2), 223–246.
Nakayama, K., 2001. Subaerial liquefied flow of volcaniclastic sediments, central Japan. In: Peakall, J., McCaffrey, B., Kneller, B. (Eds.), Sediment Transport and Deposition by Particulate Gravity Currents: International Association of Sedimentologist Special Publication, vol. 31, pp. 233–244.
Nakayama, K., Yoshikawa, S., 1997. Depositional processes of primary to reworked volcaniclastics on an alluvial plain; an example from the Lower Pliocene Ohta tephra bed of the Tokai Group, central Japan. Sedimentary Geology 107 (3–4), 211.
Ninkovich, D., 1979. Distribution, age and chemical composition of tephra layers in deep-sea sediments off western Indonesia. Journal of Volcanology and Geothermal Research 5 (1–2), 67–86.
Ninkovich, D., Shackleton, N.J., Abdel-Monem, A.A., Obradovich, J.D., Izett, G., 1978. K–Ar age of the late Pleistocene eruption of Toba, north Sumatra. Nature 276 (5688), 574–577.
Oppenheimer, C., 2002. Limited global change due to the largest known Quaternary eruption, Toba 74 kyr BP? Quaternary Science Reviews 21 (14–15), 1593–1609.
Oppenheimer, C., 2012. Eruptions that Shook the World. Cambridge University Press . (408 pp.).
Pearce, N.J.G., Bendall, C.A., Westgate, J.A., 2008. Comment on "Some numerical considerations in the geochemical analysis of distal microtephra" by A.M. Pollard, S.P.E. Blockley and C.S. Lane. Applied Geochemistry 23 (5), 1353–1364.
Petraglia, M., Korisettar, R., Boivin, N., Clarkson, C., Ditchfield, P., Jones, S., Koshy, J., Lahr, M.M., Oppenheimer, C., Pyle, D., Roberts, R., Schwenninger, J.-L., Arnold, L., White, K., 2007. Middle Paleolithic assemblages from the Indian subcontinent before and after the Toba super-eruption. Science 317 (5834), 114–116.
Petraglia, M.D., Ditchfield, P., Jones, S., Korisettar, R., Pal, J.N., 2012. The Toba volcanic super-eruption, environmental change, and hominin occupation history in India over the last 140,000 years. Quaternary International 258, 119–134.
Pyne-O'Donnell, S., 2011. The taphonomy of Last Glacial–Interglacial Transition (LGIT) distal volcanic ash in small Scottish lakes. Boreas 40 (1), 131–145.
Rampino, M.R., Self, S., 1992. Volcanic winter and accelerated glaciation following the Toba super-eruption. Nature 359 (6390), 50.
Rampino, M.R., Self, S., 1993. Climate–volcanism feedback and the Toba eruption of 74,000 years ago. Quaternary Research 40 (3), 269.
Rose, W.I., Chesner, C.A., 1987. Dispersal of ash in the great Toba eruption, 75 ka. Geology 15 (10), 913–917.
Rose, W.I., Chesner, C.A., 1990. Worldwide dispersal of ash and gases from earth's largest known eruption: Toba, Sumatra, 75 ka. Palaeogeography, Palaeoclimatology, Palaeoecology 89 (3), 269–275.
Sarna-Wojcicki, A.M., Davis, J.O., 1991. Quaternary tephrochronology. In: Morrison, R.B. (Ed.), The Geology of North America, Quaternary Nonglacial Geology: Conterminous U.S. The Geological Society of America, Boulder, Colorado, pp. 93–116.
Sarna-Wojcicki, A.M., Meyer, C.E., Bowman, H.R., Timothy Hall, N., Russell, P.C., Woodward, M.J., Slate, J.L., 1985. Correlation of the Rockland ash bed, a 400,000-year-old stratigraphic marker in northern California and western Nevada, and implications for middle Pleistocene palaeogeography of central California. Quaternary Research 23 (2), 236–257.
Schneider, J.L., Le Ruyet, A., Chanier, F., Buret, C., Ferriåre, J., Proust, J.-N.l, Rosseel, J.-B., 2001. Primary or secondary distal volcaniclastic turbidites: how to make the distinction? An example from the Miocene of New Zealand (Mahia Peninsula, North Island). Sedimentary Geology 145 (1–2), 1–22.
Schulz, H., Emeis, K.-C., Erlenkeuser, H., von Rad, U., Rolf, C., 2002. The Toba volcanic event and interstadial/stadial climates at the marine isotopic stage 5 to 4 transition in the Northern Indian Ocean. Quaternary Research 57 (1), 22–31.
Scrivenor, J.B., 1930. A recent rhyolite-ash with sponge-spicules and diatoms in Malaya. Geological Magazine 67 (9), 385–393.
Shane, P., Westgate, J., Williams, M., Korisettar, R., 1995. New geochemical evidence for the youngest Toba Tuff in India. Quaternary Research 44 (2), 200–204.
Smith, V.C., Pearce, N.J.G., Matthews, N.E., Westgate, J.A., Petraglia, M.D., Haslam, M., Lane, C.S., Korisettar, R., Pal, J.N., 2011. Geochemical fingerprinting of the widespread Toba tephra using biotite compositions. Quaternary International 246 (1–2), 97–104.
Stauffer, P.H., 1972. Cenozoic. In: Gobbett, D.J., Hutchison, C.S. (Eds.), Geology of the Malay Peninsula (West Malaysia and Singapore). : Regional Geology. John wiley and Sons, pp. 143–176.
Stauffer, P.H., 1973. Late Pleistocene age indicated for volcanic ash in west Malaysia. Geological Society of Malaysia Newsletter 40, 1–4.
Van der Kaars, S., Williams, M.A.J., Bassinot, F., Guichard, F., Moreno, E., Dewilde, F., Cook, E.J., 2012. The influence of the 73 ka Toba super-eruption on the ecosystems of northern Sumatra as recorded in marine core BAR94-25. Quaternary International 258, 45–53.
Walker, D., 1956. Studies on the Quaternary of the Malay Peninsula. Pt. I. Alluvial deposits of Perak and the relative levels of land and sea. Federal Museum Journal 1–2, 19–34.
Westgate, J.A., Perkins, W.T., Fuge, R., Pearce, N.J.G., Wintle, A.G., 1994. Trace-element analysis of volcanic glass shards by laser ablation inductively coupled plasma mass spectrometry: application to tephrochronological studies. Applied Geochemistry 9 (3), 323–335.
Westgate, J.A., Shane, P.A.R., Pearce, N.J.G., Perkins, W.T., Korisettar, R., Chesner, C.A., Williams, M.A.J., Acharyya, S.K., 1998. All Toba tephra occurrences across peninsular India belong to the 75,000 yr B.P. eruption. Quaternary Research 50 (1), 107–112.
Williams, M., 2012a. The 73 ka Toba super-eruption and its impact: history of a debate. Quaternary International 258, 19–29.
Williams, M., 2012b. Did the 73 ka Toba super-eruption have an enduring effect? Insights from genetics, prehistoric archaeology, pollen analysis, stable isotope geochemistry, geomorphology, ice cores, and climate models. Quaternary International 269, 87–93.

Williams, M.A.J., Ambrose, S.H., van der Kaars, S., Ruehlemann, C., Chattopadhyaya, U., Pal, J., Chauhan, P.R., 2009. Environmental impact of the 73 ka Toba super-eruption in South Asia. Palaeogeography, Palaeoclimatology, Palaeoecology 284 (3–4), 295–314.
Williams, M.A.J., Ambrose, S.H., der Kaars, S. v, Ruehlemann, C., Chattopadhyaya, U., Pal, J., Chauhan, P.R., 2010. Reply to the comment on "Environmental impact of the 73 ka Toba super-eruption in South Asia" by M. A. J. Williams, S. H. Ambrose, S. van der Kaars, C. Ruehlemann, U. Chattopadhyaya, J. Pal, P. R. Chauhan [Palaeogeography, Palaeoclimatology, Palaeoecology 284 (2009) 295–314]. Palaeogeography, Palaeoclimatology, Palaeoecology 296 (1–2), 204–211.
Zielinski, G.A., Mayewski, P.A., Meeker, L.D., Whitlow, S., Twickler, M.S., Taylor, K., 1996. Potential atmospheric impact of the Toba mega-eruption ~71,000 years ago. Geophysical Research Letters 23.

https://doi.org/10.1016/j.yqres.2012.11.006 Published online by Cambridge University Press